

Triple Minima in the Free Energy of Semiflexible Polymers

Abhishek Dhar¹ and Debasish Chaudhuri²

¹Raman Research Institute, Bangalore 560080, India

²S.N.Bose National Center for Basic Sciences, Calcutta 700098, India

(Received 20 October 2001; published 19 July 2002)

We study the free energy of the worm-like-chain model, in the constant-extension ensemble, as a function of the stiffness λ for finite chains of length L . We find that the polymer properties obtained in this ensemble are *qualitatively* different from those obtained using constant-force ensembles. In particular, we find that as we change the stiffness parameter, $t = L/\lambda$, the polymer makes a transition from the flexible to the rigid phase and there is an intermediate regime of parameter values where the free energy has three minima and both phases are stable. This leads to interesting features in the force-extension curves.

DOI: 10.1103/PhysRevLett.89.065502

PACS numbers: 61.41.+e

The simplest model for describing semiflexible polymers without self-avoidance is the so-called worm-like-chain (WLC) model [1–3]. In this model the polymer is modeled as a continuous curve that can be specified by a d -dimensional ($d > 1$) vector $\bar{x}(s)$, s being the distance, measured along the length of the curve, from one fixed end. The energy of the WLC model is just the energy due to curvature and is given by

$$\frac{H}{k_B T} = \frac{\kappa}{2} \int_0^L \left(\frac{\partial \hat{u}(s)}{\partial s} \right)^2 ds, \quad (1)$$

where $\hat{u}(s) = \partial \bar{x}/\partial s$ is the tangent vector and satisfies $\hat{u}^2 = 1$. The parameter κ specifies the stiffness of the chain and is related to the persistence length λ defined through $\langle \hat{u}(s) \cdot \hat{u}(s') \rangle = e^{-|s-s'|/\lambda}$. It can be shown that $\kappa = (d-1)\lambda/2$.

The thermodynamic properties of such a chain can be obtained from the free energy which can be either the Helmholtz's (F) free energy or the Gibb's (G) energy. In the former case one considers a polymer whose ends are kept at a fixed distance r [one end fixed at the origin and the other end at $\bar{r} = (0, \dots, 0, r)$] by an average force $\langle f \rangle = \partial F(r, L)/\partial r$, while in the latter case one fixes the force and the average extension is given by $\langle r \rangle = -\partial G(f, L)/\partial f$. It can be shown that in the thermodynamic limit $L \rightarrow \infty$ the two ensembles are equivalent and related by the usual Legendre transform $G = F - fr$. For a system with finite L/λ , the equivalence of the two ensembles is not guaranteed, especially when fluctuations become large. We note that real polymers come with a wide range of values of the parameter $t = L/\lambda$ [e.g., $\lambda \approx 0.1 \mu\text{m}$ for DNA while $\lambda \approx 1 \mu\text{m}$ for actin and their lengths can be varied] and fluctuations in r (or f) can be very large. Then the choice of the ensemble depends on the experimental conditions. Experiments on stretching polymers are usually performed by fixing one end of the polymer and attaching the other end to a bead which is then pulled by various means (magnetic, optical, mechanical, etc.). In such experiments either one can fix the force on the bead and measure the

average polymer extension or one can constrain the bead's position and look at the average force on the polymer. In the former case, the Gibb's free energy is relevant, while it is the Helmholtz in the second case. This point has been carefully analyzed by Kreuzer and Payne in the context of atomic force microscope experiments [4]. Theoretically, the constant-force ensemble is easier to treat, and, in fact, an exact numerical solution has been obtained [5] (though only for $t \gg 1$). Data on force-extension experiments on DNA [6] have been explained using this ensemble [5]. The case of the constant-extension ensemble turns out to be much harder and no exact solution is available. The $t \rightarrow 0$ and $t \rightarrow \infty$ cases correspond to the solvable limits of the hard rod and the Gaussian chain. The small and large t cases have been treated analytically by perturbation theory about these two limits [7–9]. Numerical simulations for different values of t have been reported by Wilhelm and Frey [10], who have also obtained series expansions valid in the small t limit. A mean-field treatment has also recently been reported [11].

In this Letter we probe the nature of the transition from the Gaussian to the rigid rod with a change of stiffness as shown by the form of the Helmholtz free energy of the WLC model (or equivalently the distribution of end-to-end distance). Extensive simulations are performed in two and three dimensions using the equivalence of the WLC model to a random walk with one-step memory. We find that, over a range of values of t , the free energy has three minima. This is verified in a one-dimensional version of the model which is exactly solvable.

We first note that the WLC model describes a particle in d dimensions moving with a constant speed (set to unity) and with a random acceleration. It is thus described by the propagator

$$Z(\bar{x}, \hat{u}, L | \bar{x}', \hat{u}', 0) = \frac{\int_{(\bar{x}', \hat{u}')}^{(\bar{x}, \hat{u})} \mathcal{D}[\bar{x}(s)] e^{-H/k_B T}}{\int \mathcal{D}[\bar{x}(s)] e^{-H/k_B T}}, \quad (2)$$

where in the numerator only paths $\bar{x}(s)$, satisfying $\bar{x}(0) = \bar{x}'$, $\bar{x}(L) = \bar{x}$, $\hat{u}(0) = \hat{u}'$, and $\hat{u}(L) = \hat{u}$, are

considered. It can be shown that the corresponding probability distribution $W(\bar{x}, \hat{u}, L)$ satisfies the following Fokker-Planck equation [7,8]:

$$\frac{\partial W}{\partial L} + \hat{u} \cdot \nabla_{\bar{x}} W - \frac{1}{2\kappa} \nabla_{\hat{u}}^2 W = 0, \quad (3)$$

where $\nabla_{\hat{u}}^2$ is the diffusion operator on the surface of the unit sphere in d dimensions. The discretized version of this model is the freely rotating chain (FRC) model of semiflexible polymers [1]. In the FRC one considers a polymer with N segments, each of length $b = L/N$. Successive segments are constrained to be at a fixed angle, θ , with each other. The WLC model is obtained, in the limit $\theta, b \rightarrow 0, N \rightarrow \infty$ keeping $\lambda = 2b/\theta^2$ and $L = Nb$ finite.

Here we will consider the situation where the ends are kept at a fixed separation r [with \bar{x} at the origin and $\bar{x} = \bar{r} = (0, \dots, 0, r)$], but there is no constraint on \hat{u} and \hat{u}' and they are taken as uniformly distributed. Thus we will be interested in the distribution $P(r, L) = \langle \delta(\bar{x} - \bar{r}) \rangle = \int d\hat{u} W(\bar{r}, \hat{u}, L)$: this gives the Helmholtz free energy $F(r, L) = -\log[P(r, L)]$. For the spherically symmetric situation we are considering, $P(r, L)$ is simply related to the radial probability distribution $S(r, L)$ through $S(r, L) = Cr^{d-1}P(r, L)$, C being a constant equal to the area of the d -dimensional unit sphere. It may be noted that the WLC Hamiltonian is equivalent to spin $O(d)$ models in one dimension in the limit of the exchange constant $J \rightarrow \infty$ (with $Jb = \kappa$ finite) and all results can be translated into spin language. However, for spin systems, the present free energy is not very relevant since it corresponds to putting unnatural constraints on the magnetization vector.

Numerical simulations.—The simulations were performed by generating random configurations of the FRC

$$\begin{aligned} \langle r^2 \rangle &= \frac{4\kappa L}{d-1} - \frac{8\kappa^2(1 - e^{-\frac{(d-1)L}{2\kappa}})}{(d-1)^2} \\ \langle r^4 \rangle &= \frac{64\kappa^4(d-1)}{d^3(d+1)^2} e^{-\frac{dL}{\kappa}} - \frac{128\kappa^4(d+5)^2}{(d-1)^4(d+1)^2} e^{-\frac{(d-1)L}{2\kappa}} + \frac{64\kappa^3L(d^2 - 8d + 7)}{(d-1)^4(d+1)} e^{-\frac{(d-1)L}{2\kappa}} + \frac{64\kappa^4(d^3 + 23d^2 - 7d + 1)}{(d-1)^4d^3} \\ &\quad - \frac{64\kappa^3L(d^3 + 5d^2 - 7d + 1)}{(d-1)^4d^2} + \frac{16\kappa^2L^2(d^3 - 3d + 2)}{d(d-1)^4}. \end{aligned} \quad (4)$$

In fact, it is straightforward to compute all even moments, though it becomes increasingly tedious to get the higher moments. Our numerics agrees with the exact results to around 0.1% for $\langle r^2 \rangle$ and 0.5% for $\langle r^4 \rangle$.

The function P has the scaling form $P(r, L) = \frac{1}{L^d} p(r/L, L/\lambda)$ and we will focus on determining the function $p(v, t)$ [13]. In Figs. 1 and 2, we show the results of our simulations in two and three dimensions. At large values of t there is a single maximum at $v = r/L = 0$ corresponding to a Gaussian distribution, while at small t the maximum is close to the fully extended value of $v = \pm 1$. The transition is *first-order-like*: as we decrease t , at some critical value, p develops two additional maxima at nonzero values of v . Further decreasing t weakens

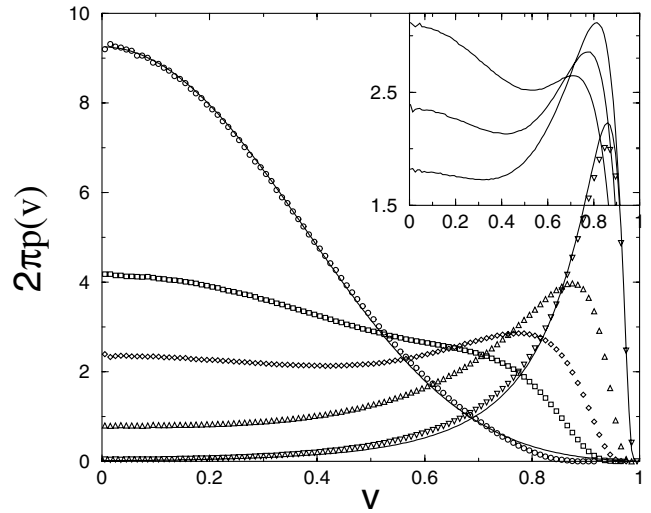


FIG. 1. Monte Carlo data for $p(v, t)$ for the two-dimensional WLC for values of $t = 10$ (\circ), 5, 3.33, 2, and 1 (∇). The inset is a blowup of curves in the transition region ($t = 4, 3.33, 2.86$) and clearly shows the presence of the two maxima. Note that because of $\pm v$ symmetry, we have plotted data for positive v values only. For the fits at large and small t see text.

model and computing the distribution of end-to-end distances. To obtain equivalence with the WLC model the appropriate limits were taken. We note that, because these simulations do not require equilibration, they are much faster than simulations on equivalent spin models and give better statistics. The number of configurations generated was around 10^8 for chains of size $N = 10^3$. Increasing N did not change the data significantly. As a check on our numerics we evaluated $\langle r^2 \rangle$ and $\langle r^4 \rangle$. Using Eq. (3) and following [12] we can compute these (in all dimensions):

the maximum at $v = 0$ until it finally disappears and there are just two maxima which correspond to the rigid chain.

For the limiting cases of small and large values of t there are analytic results for the distribution function, and, as can be seen in Figs. 1 and 2, our data agree with them. For large t we find that Daniels' approximation [7], which is a perturbation about the Gaussian, fits the data quite well. In the other limit of small t the series solutions provided in [10] fit our data. For intermediate values of t neither of the two forms are able to capture, even qualitatively, the features of the free energy. Specifically, we note that all the analytic theories (perturbative, series expansions, and

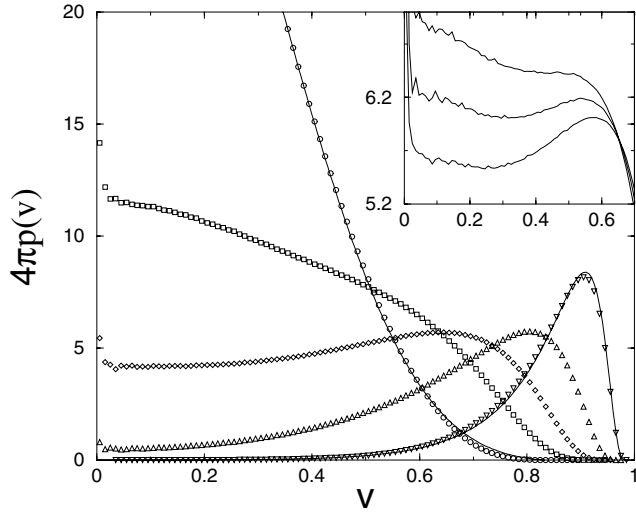


FIG. 2. Monte Carlo data for $p(v, t)$ for the three-dimensional WLC for values of $t = 10$ (○), 5, 3.33, 2, and 1 (∇). The inset is a blowup of curves in the transition region ($t = 4, 3.85, 3.7$) and shows the presence of the two maxima.

mean-field) predict a second-order-like transition and do not give the triple minima for any parameter value.

It is instructive to study a one-dimensional version of the WLC which shows the same qualitative features (the equivalent spin problem is the Ising model). Consider a N step random walk, with step-size b which, with probability ϵ , reverses its direction of motion and, with $1 - \epsilon$, continues to move in the same direction. The appropriate

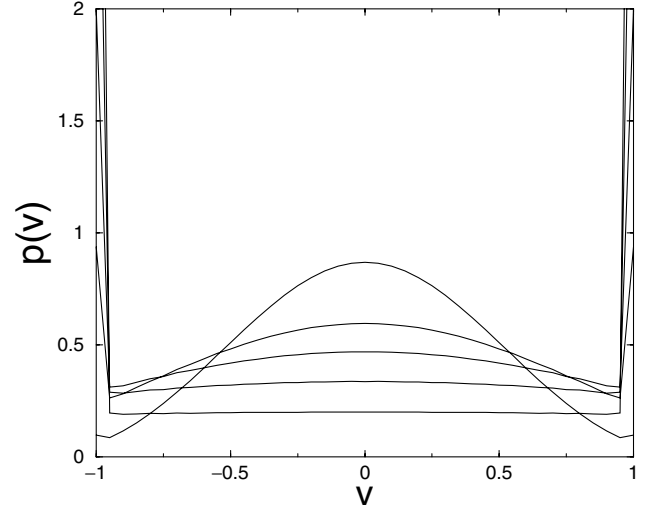


FIG. 3. The exact distribution $p(v, t)$ of the one-dimensional WLC [Eq. (6)] for different values of t (10, 5, 3.33, 2, 1). Even for the stiffest chain considered here ($t = 1$), the distribution has a peak at the center (in addition to the δ -function peaks at ends) though it looks flat.

scaling limit is $b \rightarrow 0$, $\epsilon \rightarrow 0$, $N \rightarrow \infty$ keeping $L = Nb$, $t = L/\lambda = 2N\epsilon$ finite. Defining $Z_{\pm}(x, L)$ as the probability of the walker to be at x with either positive or negative velocity, we have the following Fokker-Planck equation:

$$\frac{\partial Z_{\pm}}{\partial L} = \mp \frac{\partial Z_{\pm}}{\partial x} \mp \frac{1}{2\lambda} (Z_{+} - Z_{-}). \quad (5)$$

This can be solved for $P(x, L) = Z_{+} + Z_{-} = \frac{1}{L} p(x/L, L/\lambda)$. We get

$$p(v, t) = \frac{te^{-t/2}}{4} \left[\frac{I_1\left(\frac{t}{2}\sqrt{1-v^2}\right)}{\sqrt{1-v^2}} + I_0\left(\frac{t}{2}\sqrt{1-v^2}\right) \right] + \frac{e^{-t/2}}{2} [\delta(v-1) + \delta(v+1)], \quad (6)$$

where I_0 and I_1 are modified Bessel functions. In Fig. 3 we have plotted $p(v, t)$ for different values of stiffness. We find that it always has three peaks. Unlike in two and three dimensions, the δ -function peaks at $v = \pm 1$ (which corresponds to fully extended chains) persist at all values of stiffness though their weight decays exponentially. Similarly, the peak at $v = 0$ is always present.

Discussion.—The most interesting result of this paper is the triple minima in the Helmholtz free energy of the WLC. Physically, this results from the competing effects of entropy, which tries to pull in the polymer, and the bending energy, which tries to extend it. This form of the free energy leads to a highly *counterintuitive force-extension curve*, very different from what one obtains from the constant-force ensemble or from approximate theories. In Fig. 4 we show the force-extension curve for a two-dimensional chain with $t = 3.33$. We see that there are two stable positions for which the force is zero. In the constant-force ensemble, it is easy to show that $\partial\langle r \rangle / \partial f = \langle r^2 \rangle - \langle r \rangle^2$ and so the force extension is always monotonic. In the constant-extension ensemble, there is no analogous

result (for finite systems), and monotonicity is not guaranteed.

Most recent experiments on stretching DNA have $t \geq 100$. The distribution is then sharply peaked at zero, and one expects the equivalence of different ensembles. Experimentally the value of t can be tuned by various means, for example, by changing the length of the polymer or the temperature. Polymer-stretching experiments can thus be performed for intermediate t values. Since we consider the tangent vectors at the polymer ends to be unconstrained, an accurate experimental realization of our setup would be one in which both ends are attached to beads (see Fig. 5). The beads are put in optical traps and so are free to rotate (this setup is identical to the one used in Ref. [14]). Making the traps stiff corresponds to working in the constant-extension ensemble [4], and one can measure the average force. Our predictions can then be experimentally verified. We make some estimates on the experimental requirements (for a 3D polymer with stiffness $t = 3.85$). Assume that at one end, the origin, the trap is so

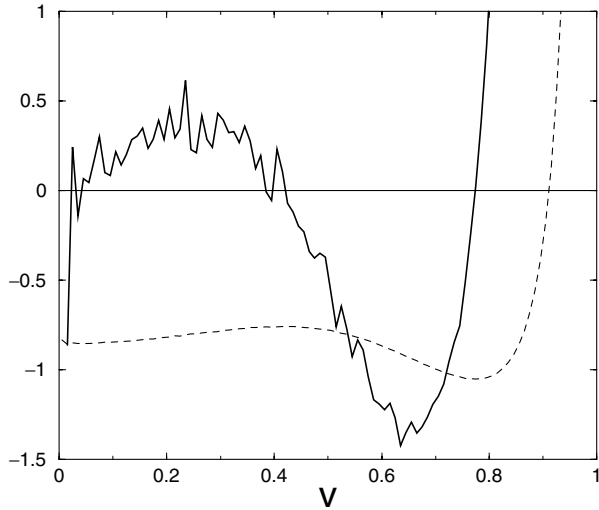


FIG. 4. The free energy (dotted line) and the corresponding force-extension curve (solid line) for a two-dimensional chain with $t = 3.33$.

stiff that the bead can only rotate. We make measurements at the other end. The trap center is placed at $\bar{r}_0 = (0, 0, z_0)$ and the mean bead displacement $\Delta z = \langle (z - z_0) \rangle$ gives the mean force $\langle f \rangle$ on the polymer. We then consider the problem of the polymer in the presence of a trap potential $V = [k_t(x^2 + y^2) + k(z - z_0)^2]/2$. Assume $k_t \gg k$ so we can neglect transverse fluctuations. The distribution of the bead's position in the presence of the potential is given by $Q(\bar{r}) = e^{-\beta[F(\bar{r})+V(\bar{r})]} / \int d^3\bar{r} e^{-\beta[F(\bar{r})+V(\bar{r})]}$. For a stiff trap, we can expand F about $\bar{r} = \bar{r}_0$ and find that the average displacement of the bead is given by $\Delta z = \int d^3\bar{r} (z - z_0) Q(\bar{r}) = -\langle f \rangle / k'$, where $k' = k + F''(z_0) \approx k$ (valid except when $z_0 \approx L$) and $\langle f \rangle = F'(z_0)$. The rms fluctuation of the bead about the trap center is given by $z_{\text{rms}}^2 = k_B T / k$. Hence we get $\Delta z = -\langle f \rangle z_{\text{rms}}^2 / (k_B T) = -(\langle f \rangle L / k_B T) (z_{\text{rms}}^2 / L)$. The scaled force $\langle f \rangle L / (k_B T)$ is of order 0.1. The different minima are separated by distances $\approx 0.2L$; hence, to see the effect we need to have $z_{\text{rms}} / L \lesssim 0.1$. Thus, finally we find that the typical displacement of the bead Δz is about $0.01 z_{\text{rms}}$. This is quite small and means that it is necessary to collect data on the bead position over long periods of time.

As suggested in [10], a more direct way of measuring the Helmholtz free energy would be to attach marker molecules at the ends of the polymer and determine the distribution of end-to-end distances. Fluorescence microscopy as in [15] could be another possible method. It is to be remembered, of course, that real polymers are well modeled by the WLC model, provided we can neglect monomer-monomer interactions (steric, electrolytic, etc.). Thus the experiments would really test the relevance of the WLC model in describing real semiflexible polymers in different stiffness regimes.

In conclusion, we have presented some new and interesting properties of the WLC model and have pointed out that polymer properties are ensemble dependent. We have given one example of qualitative differences in force-

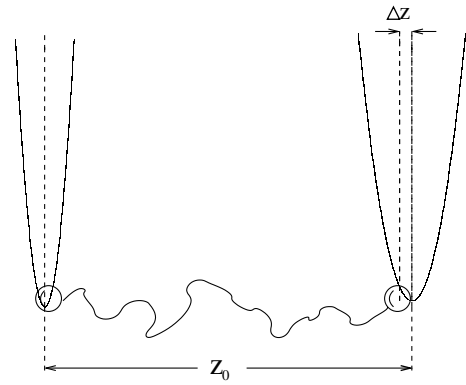


FIG. 5. A schematic of the experimental setup required to realize the constant-extension ensemble discussed in the paper (see Ref. [14]). For a stiff trap the average displacement of the bead $\langle \Delta z \rangle$ from the trap center is small, and the average force on the polymer is $\langle f \rangle = -k \langle \Delta z \rangle$.

extension measurements in different ensembles. Other quantitative differences will occur even in more flexible chains and should be easier to observe experimentally. We hope this work will motivate further experimental and theoretical work on this simplest model for semiflexible polymers.

We thank O. Narayan and J. Samuel for discussions. One of us (D.C.) thanks CSIR, India, for support.

Note added.—After submission of this paper, an exact numerical solution of the WLC model has been obtained and has reproduced our results [16].

- [1] M. Doi and S.F. Edwards, *The Theory of Polymer Dynamics* (Clarendon, Oxford, 1992).
- [2] N. Saito, K. Takahashi, and Y. Yunoki, *J. Phys. Soc. Jpn.* **22**, 219 (1967).
- [3] E. Frey *et al.*, cond-mat/9707021.
- [4] H.J. Kreuzer and S.H. Payne, *Phys. Rev. E* **63**, 021906 (2001).
- [5] J.F. Marko and E.D. Siggia, *Macromolecules* **28**, 8759 (1995).
- [6] S.B. Smith, L. Finzi, and C. Bustamante, *Science* **258**, 1122 (1992).
- [7] H.E. Daniels, *Proc. R. Soc. Edinburgh, Sect. A: Math. Phys.* **63A**, 290 (1952).
- [8] W. Gobush *et al.*, *J. Chem. Phys.* **57**, 2839 (1972).
- [9] T. Norisuye, H. Murakama, and H. Fujita, *Macromolecules* **11**, 966 (1978).
- [10] J. Wilhelm and E. Frey, *Phys. Rev. Lett.* **77**, 2581 (1996).
- [11] D. Thirumalai and B. Y. Ha, cond-mat/9705200.
- [12] J.J. Hermans and R. Ullman, *Physica* **18**, 951 (1952).
- [13] Wilhelm and Frey [10] have looked at the radial distribution $S(r, L)$ which, however, misses the interesting details of the transition. We note that the relevant distribution here is indeed $p(v, t)$ since this gives the Helmholtz free energy.
- [14] J.-C. Meiners and S.R. Quake, *Phys. Rev. Lett.* **84**, 5014 (2000).
- [15] A. Ott *et al.*, *Phys. Rev. E* **48**, R1642 (1993).
- [16] J. Samuel and S. Sinha, cond-mat/0203483.